Identification of the Residues in the Helix F/G Loop Important to Catalytic Function of Membrane-Bound Prostacyclin Synthase†

Hui Deng, Jiaxin Wu, Shui-Ping So, and Ke-He Ruan*

The Vascular Biology Research Center and Division of Hematology, Department of Internal Medicine, The University of Texas Health Science Center, Houston, Texas 77030

Received August 27, 2002; Revised Manuscript Received February 14, 2003

ABSTRACT: A topological model of prostaglandin I_2 synthase (PGIS) was created by homology modeling. This model, along with site-specific antibodies and other topology studies, has suggested that the residue(s) within helix F/G loop of PGIS may be involved in forming the substrate access channel and located in a position that influences the membrane-bound PGIS catalytic function (*1*). To test this hypothesis, we have explored an approach to identify the residues of the helix F/G loop important to enzyme activity of the membrane-bound PGIS by a combination of 2-D NMR experiment and mutagenesis methods. Using the distance measured from the model as a guide, the helix F/G loop was mimicked in a synthetic peptide by introducing a spacer to maintain a distance of about 7 Å between the N- and the C-termini (PGIS residues 208 and 230). The peptide was used to interact with the enzyme substrate analogue, U46619. High-resolution 2-D NMR experiments were performed to determine the contacts between the peptide and U46619. The interaction between the constrained F/G loop peptide and U46619 was confirmed by the observation of the conformational changes of the peptide and U46619 using the comparison of the cross-peaks between the NOESY spectra of U46619 with the peptide, without the peptide, and the peptide alone. Through the combination of the 2-D NMR experiments, completed ^{1}H NMR assignments of the F/G loop segment in the presence and absence of U46619 were obtained, and these data were used to predict the contact residues (Leu214 and Pro215) of the F/G loop with PGIS substrate. The predicted influence of residues on enzyme catalytic activity in membrane-bound environments was confirmed by the mutagenesis of the F/G loop residues of human PGIS. These observations support that the F/G loop is involved in forming the substrate access channel for membrane-bound PGIS and suggests that the NMR experiment-based mutagenesis approach may be applied to study structure and function relationships for other proteins.

Prostaglandin I_2 synthase (PGIS),[1] one of the eicosanoids-synthesizing P450s, is located in the endoplasmic reticulum (ER) membrane where prostaglandin H_2 (PGH_2) is converted to prostaglandin I_2 (PGI_2), a potent inhibitor of platelet aggregation, vasoconstriction, and leukocyte interactions with endothelium (*2*, *3*). In the ER membrane, PGI_2 biosynthesis requires efficient coordination between PGIS and prostaglandin H_2 synthase (PGHS) to produce PGIS substrate, PGH_2. Results from crystallography and topology studies have indicated that the catalytic domain of PGHS is located on the luminal side of the ER (*4*−*6*). The PGHS lipid substrate, arachidonic acid (AA), thus appears to be delivered to its cyclooxygenase channel via the ER lipid bilayer. Our peptidoliposome reconstitution and circular dichroism (CD) spectroscopy studies of the PGIS NH_2-terminal membrane domain concluded that the PGIS NH_2-terminal membrane anchor domain is similar to other microsomal P450s (*7*). Current studies using modeling-guided site-specific antibodies have indicated that peptide segments in different surface regions of PGIS are exposed on the cytoplasmic side of the ER membrane (*8*). The data support a topological arrangement of PGIS, in which the bulk of the eicosanoid-synthesizing P450 protein lies on the outside of the ER bilayer and is anchored to the ER membrane by its hydrophobic NH_2-terminal domain. The PGIS substrate, PGH_2, thus needs to be delivered from the ER lumen to the substrate binding site of PGIS on the cytoplasmic side through the substrate access channel via the ER lipid bilayer. To test whether the PGIS substrate access opening is near the ER membrane, our very current studies prepared a series of site-specific antibodies against peptide segments predicted to be near the surface of the substrate access channel. The results indicated that peptide segments in the surrounding surface could be accessed by their antibodies with the protein still anchored in the membrane. However, surface peptide segments immediately on the mouth of the substrate channel were accessible only after the membrane was solubilized with detergent (*1*). These data suggest that the PGIS substrate access channel opening is close to, and shielded by, the ER membrane. With this information, we have built a membrane

† This work was supported by NIH Grants HL56712 and NS 23327.

* To whom correspondence should be addressed. Tel.: (713) 500-6769. Fax: (713) 500-6810. E-mail: kruan@uth.tmc.edu.

[1] Abbreviations: PGIS, prostaglandin I_2 synthase; ER, endoplasmic reticulum; NMR, nuclear magnetic resonance; 2-D, two-dimensional; NOESY, nuclear Overhauser effect spectroscopy; TOCSY, total correlation spectroscopy; DQF-COSY, double-quantum filtered correlation spectroscopy; PGHS, prostaglandin H_2 synthase; CD, circular dichroism; HPLC, high performance liquid chromatography.

10.1021/bi026749z CCC: $25.00
Published on Web 04/22/2003

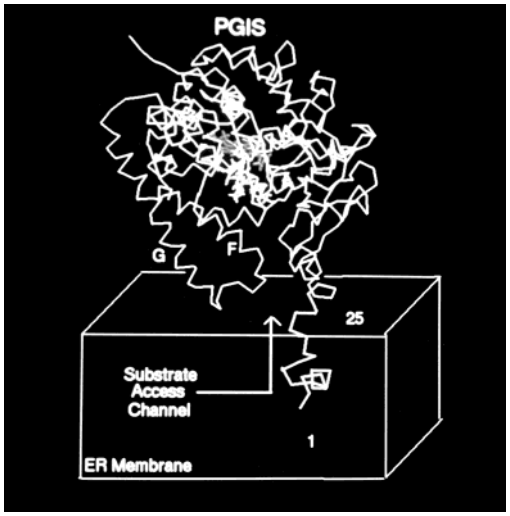

FIGURE 1: Putative overall topology of PGIS with respect to the ER membrane. NMR 3-D structure of the NH_2-terminal membrane anchor domain of human PGIS (residues 1−25) was grafted on to the PGIS 3-D structural working model constructed by homology modeling using P450BM3 as a template (*1*, *8*). It was then inserted into the ER membrane with the NH_2-terminal hydrophobic residues (*1*). The helix F/G loop contacted with the membrane proposed was labeled with letters.

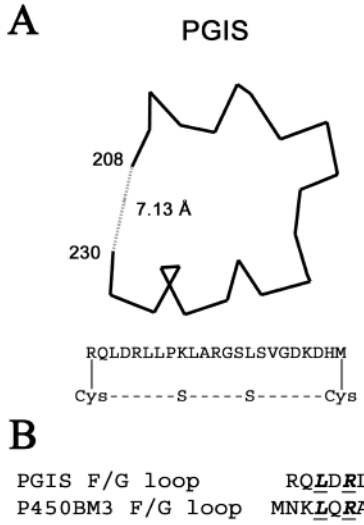

FIGURE 2: (A) Detailed view of the F/G loop of the PGIS working model. The measurement of N- and C-termini of the loop was shown by the dotted line, and the distance was indicated. The amino acid sequence of the synthetic peptide corresponding to the F/G loop was shown in cyclic form, which had a connection between the N- and the C-termini using a disulfide bound by additional cysteine residues at the termini. (B) Sequence alignment of the F/G loops of PGIS and P450BM33. The identical residues in the F/G loops were underlined.

topological arrangement model for PGIS, suggesting that the helix F/G loop may also contact the ER membrane and be involved in forming the substrate access channel (Figure 1).

In the membrane-bound PGIS model, the helix F/G loop is in a position that influences the orientation of the substrate access channel in respect to the ER membrane (Figure 1). Thus, characterization of the helix F/G loop has become a key step in further defining the PGIS substrate channel orientation and the influences of the F/G loop on the enzyme catalytic activity. In this paper, we have identified several residues within the helix F/G loop that are important to the catalytic activity of membrane-bound PGIS by an approach of 2-D NMR experiment-guided mutagenesis, and this paper also suggests that the residues are involved in forming the PGIS substrate access channel.

MATERIALS AND METHODS

Peptide Synthesis. A peptide corresponding to the F/G loop of PGIS (residues 208−230) with an additional cysteine residue added at both ends of the loop was synthesized using fluorenylmethoxycarbonyl-polyamide solid-phase method. After cleavage with TFA, the peptide was purified to homogeneity by HPLC on a Vydac C4 reversed phase column with a gradient from 20−80% acetonitrile in 0.1% TFA. The purified peptide was dissolved in water at a final concentration of 0.02 mg/mL. The solution was adjusted to pH 8.5 using triethylamine and stirred overnight at room temperature for cyclization of the peptide. The cyclic peptide was then lyophilized and purified on Sephadex G-25 column. The sequence of the synthesized PGIS F/G loop peptide is shown in Figure 2A.

NMR Experiments. The cyclic PGIS F/G loop peptide was dissolved in 20 mM, pH 5.5 sodium phosphate buffer at a final concentration of 4 mM (10% D_2O for H_2O experiments and 100% D_2O for D_2O experiments) and used for the NMR experiments. DQF-COSY, TOCSY, and NOESY spectra were acquired on a Bruker AMXII-600 spectrometer at 293 K. NOESY spectra were recorded with mixing time of 150, 250, and 350 ms, and TOCSY spectra were carried out using a MLEV-16 spin-lock sequence with a total mixing time of 80 ms. The DQF-COSY spectrum was composed of 4096 complex points in F2. The TOCSY and NOESY spectra were composed of 2048 complex points with 64 scans per t1 increment of a total of 512 t1 increments were used. Quadrature detection in F1 was achieved by the TPPI method. The water peaks defined as 4.72 ppm were used as a reference for chemical shifts. The NMR data was processed using the Felix program (Molecular Simulation, Inc., San Diego, CA). All FIDs were zero-filled to 2048 × 2048 before Fourier transformation, and 0° (for DQF-COSY) or 60° (for TOCSY and NOESY) shifted sinbell window functions were used in both dimensions. The resonance assignment of the peptide was obtained using a standard sequential assignment strategy (*9*). For the NMR experiments of the F/G loop peptide in the presence of U46619, 1 mg of U46619 was added in the above peptide solution.

Cell Culture. COS-1 cells were cultured in the 100 mm cell culture dish with high glucose Dulbecoo's modified Eagle's medium (DMEM) containing 10% fetal bovine serum and grown at 37 °C in a humidified 5% CO_2 incubator. The transfection experiment was carried out by applying 15 μg of human PGIS cDNA with 8 mg of DEAE-Dextran in 2.5 mL of DMEM to 60−70% confluent COS-1 cell. After 1-h incubation at 37 °C, 7 mL of DMEM containing 10% fetal bovine serum and 300 μg of chloroquine were added. Five hours later, the medium was changed to DMEM containing 10% fetal bovine serum with antibiotic and antimycotic for another 48-h culture.

Western Blot. The transfected COS-1 cells were scraped from the plates into ice-cold PBS buffer, pH 7.4, and collected by centrifugation. After washing three times, the pellet was resuspended in a small volume of the same buffer. The protein was separated by 10% polyacrylamide gel

electrophoresis under denaturing conditions and then transferred to a nitrocellulose membrane. A band recognized by particular primary antibodies was visualized with horseradish peroxidase substrate as described previously (*1*).

Site-Directed Mutagenesis. The full-length PGIS mutants were amplified by a one step polymerase chain reaction (PCR). The basic procedure utilized an expression vector pcDNA3.1, with wild-type PGIS as the template and two synthetic oligonucleotide primers containing the desired mutation for each reaction. The primers, each complementary to opposite strands of the template, extended during temperature cycling of 95 °C for 30 s, 52 °C for 1 min 30 s, and 68 °C for 13 min for a total of 20 cycles with an additional extension cycle of 68 °C for 10 min by using Pfu Turbo DNA polymerase (Stratagene). Following temperature cycling, the product was treated with DpnI endonuclease (Stratagene), which was used to digest the parental DNA template and to select the mutation containing synthesized cDNA. The oligonucleotide primers used for the mutations were (in 5′ to 3′ direction with mutated bases underlined):

LDR210−212MNK, CACCTTTCGCCAGATGAACAAGCTGCTCCCC; LP214−215QR, CGACCGGCTGCAACGCAAACTGGCCC; KLA216−218ANP, GCTGCTCCCCGCAAATCCCCGTGGCTC; RGS219−221DDP, CCAAACTGGCCGATGACCCCCTGTCAGTG; LSVG222−225AYDE, cccgTGGCTCCGCGTATGATGAGGACAAGGACCAC; L210M, CCTTTCGCCAGATGGACCGGCTGCTCC; D211N, CTTTCGCCAGCTCAACCGGCTGCTCC; R212K, CCAGCTCGACAAGCTGCTCCCC; L214Q, CGACCGGCTGCAACCCAAACTGGC; P215R, CGGCTGCTCCGCAAACTGGCCC; K216A, GCTGCTCCCCGCACTGGCCCGTG; L217N, CTGCTCCCCAAAAACGCCCGTGGCTCC; A218P, CCCCAAACTGCCCCGTTGGCTC; R219D, CCAAACTGGCCGATGGCTCCCTGTC; G220D, CTGGCCCGTGACTCCCTGTCAGT; and S221P, GCCCGTGGCCCCCTGTCAGT. The mutants were verified by DNA sequencing. The plasmids for transfection were prepared using a Qiagen Midiprep kit.

Thin-Layer Chromatography (TLC) for Enzymatic Assay. PGIS activity was assayed by mixing 80 μg of whole transfected or untransfected COS-1 cell pellet in PBS, 5.5 μg of purified PGH_2 synthase (provided from Dr. A.-L. Tsai), and 0.25 mM heme. [^{14}C]-Arachidonic acid (10 μM) was added in the mixture with a total reaction volume of 100 μL. After 1 min, the reaction was stopped by adding 40 μL of methanol and 1 M of citric acid (4:1 v/v). Organic products generated were extracted with 400 μL of diethyl ether twice, and 500 μL of the extract was transferred into a collection tube containing a thin layer of anhydrous sodium sulfate on the bottom. A total of 80−100 μL of the organic products were applied to a TLC plate that was chilled on ice before being placed in a developing tank. The tank was equilibrated with an organic phase of ethyl acetate/2,2,4-trimethylpentane/acetic acid/water (110:50:20 v/v/v upper phases) that had been presaturated with water. After development, the radioactive signal of [^{14}C]6-keto-$PGF_{1\alpha}$, which reflects the amount of PGI_2 converted from PGH_2 on the TLC plate, was autoradiographed and quantitatively identified by using a scanner with photoshop and Scion Image program. The position of 6-keto-$PGF_{1\alpha}$ on the TLC plate was located by comigration of the sample and the nonlabeled 6-keto-$PGF_{1\alpha}$, which was combined with iodine vapor and revealed the stained areas.

Table 1: Proton Chemical Shifts for U46619

	U46619 only (ppm)	U46619 + PGIS F/G loop (ppm)
H2	2.17	
H3	1.59	1.55
H4	2.07	2.11
H5	5.44	5.42
H6	5.45	5.42
H7/H7′	2.26/2.17	2.28/2.37
H8	1.73	1.70
H9	2.53	2.52
H10a/H10b	1.60/1.74	1.68/1.74
H11	4.11	4.11
H12	1.99	1.99
H13	5.43	5.41
H14	5.43	5.41
H15	4.02	4.00
H16	1.53/1.39	1.55
H17	1.54/1.44	1.43
H18	1.24/1.23	1.25
H19	1.26	
H20	0.86	
$_1$HC	3.54	3.55
$_2$HC	3.87	3.87

RESULTS

Design and Synthesis of a Peptide Mimicking the PGIS F/G Loop Domain. One of the key factors in mimicking a native protein's functional segment is to design a peptide fragment having similar secondary and 3-D structures to the targeted portion of the protein. On the basis of our 3-D working model of PGIS (Figure 1), the putative membrane contact region of the helix F/G loop was mimicked in a peptide by introducing a spacer (a disulfide bound) to maintain the distance of about 7 Å between the N- and C-termini (residues 208 and 230 for PGIS), matching the distance measured from the model (Figure 2A). The constrained peptide corresponding to the F/G loop region was HPLC-purified to homogeneity, and the correct mass of the peptide was confirmed by mass spectrometry analysis (data not shown).

NMR Assignment of U46619 and the F/G Loop Peptide. The proton resonance assignments for the PGH_2 analogue, U46619, in the absence and presence of the constrained F/G loop peptide were accomplished using the standard sequential assignment technique based on the proton chemical shifts (*9*−*13*). The assignment procedures involved the identification of spin systems using TOCSY spectra (data not shown) (*13*−*15*) and sequential assignment using NOESY spectra (*13*, *16*). The complete proton resonance assignments for U46619 with and without the peptide were summarized in Table 1. The identification of the interproton NOE cross-peaks was used to further construct the 3-D structures and showed the detailed structural differences of the analogue in the absence and presence of the F/G loop peptide. The assignment for the constrained F/G loop peptide in the presence of the U46619 (bound form) was performed by the same assignment strategy for the free constrained F/G loop peptide (free form) and other synthetic peptides as described (*17*−*20*). The chemical shifts assigned from the TOCSY spectrum (not shown) and the NOESY walk in the NH/αH

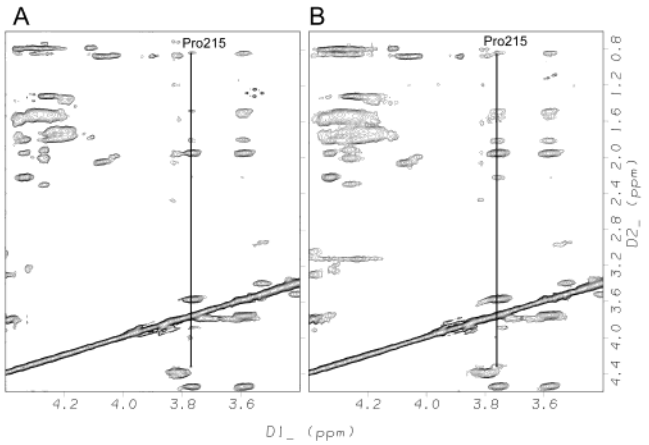

FIGURE 3: Expanded region of the NOESY spectra of the PGIS F/G loop without (A) and with (B) U46619. The intensities of the cross-peaks from the side chains of Pro215 were increased as indicated upon the addition of U46619.

region (not shown) of the NOESY spectrum for the bound form of the F/G loop peptide was similar to the free form of the peptide (*17*). The quantitative differences of the cross-peaks on the NOESY spectrum that affected the structural calculations were mainly found for the side chain of Pro215 (Figure 3). After completing the manual assignment, the accuracy of the assignment was double checked and revised, if needed, by an auto-assignment strategy using the Felix Auto-assign program (*18*−*20*).

3-D Solution Structure of U46619. The NOE cross-peak volumes assigned from the NOESY spectra of U46619 described above were converted using restricted distance of H2 and H3 of the analogues as a standard (*13*) into the upper bound of the interproton distances as NOE constraints by the Auto-assignment program within the Felix 2000 package. These obtained NOE constraints were then used for the structural calculation. Nineteen NOE constraints from the NOESY spectrum of U44069 alone and 16 NOE constraints for U46619 in the presence of the F/G loop peptide, including two inter-side chain NOEs (H4/H15 and H5/H13), were used as distance restraints for the structural calculation based on the initial structures created by the Biopolymer program within the Insight II package (*13*). The calculation included energy minimization that was carried out using NOE constraints with the distance range and the force set to 0.1 Å and 800, respectively. The constructed 3-D structural models of U46619 in the absence and presence of the F/G loop peptide were then used to run dynamics, which provided the simulation of the motion of atoms at the temperature of 300 K (room temperature) and the force of 80. After 2000 iterations, 10 3-D structural models of U46619 were built (Figure 4). The 10 conformations of U46619 in free (Figure 4A) and bound (Figure 4B) forms were superimposed for comparison (Figure 4C).

3-D Solution Structure of the Bound Form of the Constrained F/G Loop Peptide. The NOE cross-peak volumes assigned from the NOESY spectra of the bound form of the constrained F/G loop peptide described above were converted into upper bounds of the interproton distances as NOE constraints by the Auto-assignment program within the Felix 2000 package. By comparison of the constraint files of the bound form with the free form (*17*) of the F/G loop peptides, the main differences of the constraints were observed within the side chains of the Pro215. The differences are expected to change the conformation of the bound form of the peptide in the region as compared to the free form of the peptide. The 3-D structure of the bound form of the F/G loop peptide was constructed by DGII and dynamic calculations using

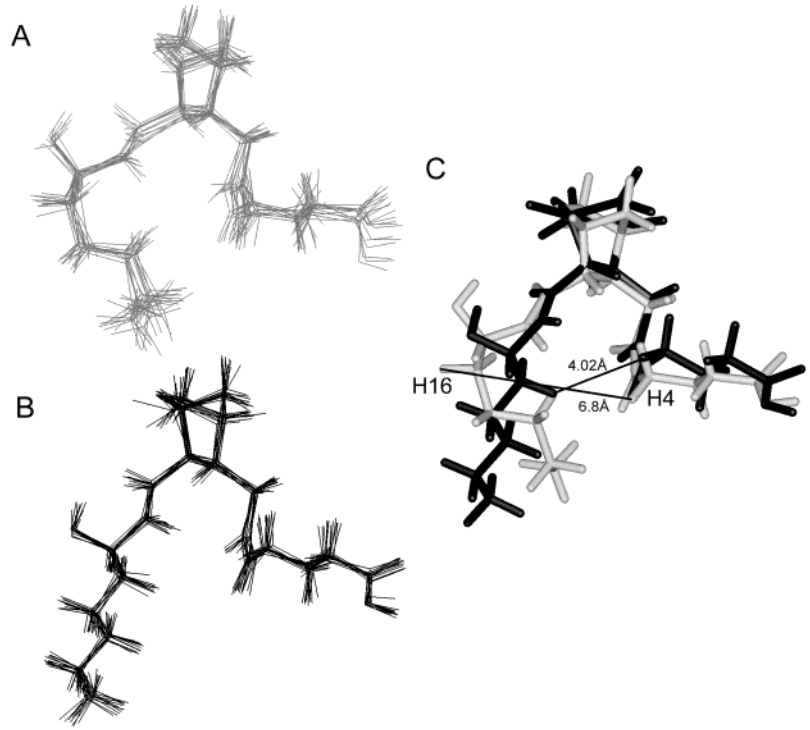

FIGURE 4: Ten 3-D structures of U46619 in the absence (A) and presence (B) of the PGIS F/G loop were obtained by dynamic studies using the corresponding cross-peak constraints from the NOESY spectra. (C) Superimposition of the 3-D structures of U46619 in the presence (dark) and absence (light) (*13*) of the PGIS F/G loop peptide. The distance between H4 and H16 was changed from 6.8 to 4.02 Å after the addition of the peptide.

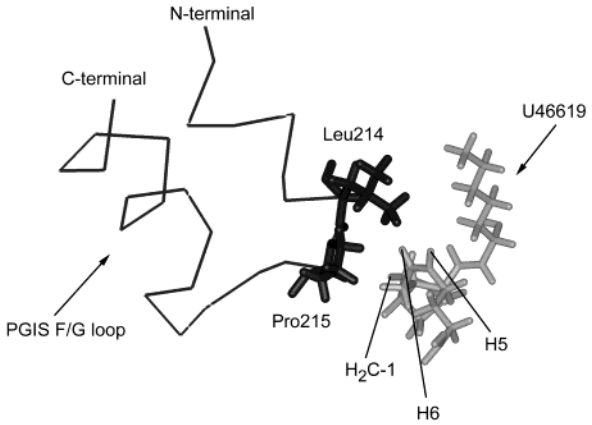

FIGURE 5: 3-D structure of the PGIS F/G loop in the presence of U46619 obtained by DGII and dynamic calculations. The molecule displayed only the α-carbons. The side chains of the particular residues of the peptide that interacted with U46619 were indicated.

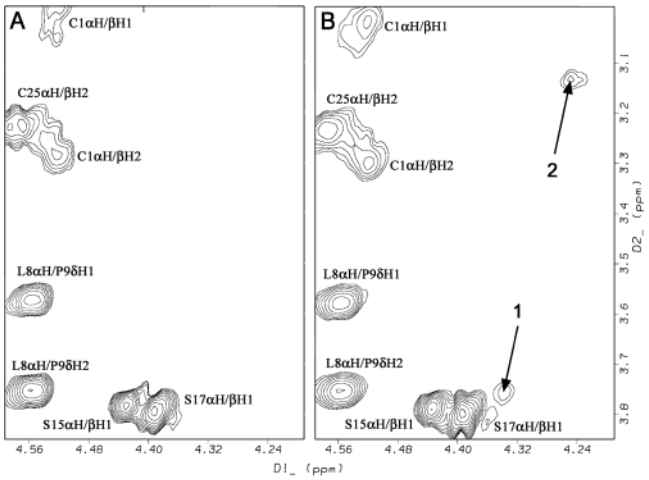

FIGURE 6: Expanded region of the NOESY spectra of the PGIS F/G loop without (A) and with (B) U46619. The assigned additional cross-peaks upon the addition of U46619 were indicated as Pro9 (PGIS Pro215αH/δ_2H) (1) and Arg13 (PGIS Arg219αH/δ_1H) (2).

all the NOE constraints obtained from the NOESY spectrum as described above (Figure 5).

Investigation of the Interaction between the F/G loop of PGIS and the Substrate Analogue, U46619, Using a 2-D NMR Technique. The first evidence is the conformational change of U46619 upon the interaction with the PGIS helix F/G loop. The distance between H4 and H16 of U46619 was changed from 6.8 to 4.02 Å after the addition of the PGIS F/G loop peptide (Figure 4C). This result clearly indicated that U46619 was able to interact with the F/G loop peptide in the given conditions. Next, the interaction of the F/G loop peptide with U46619 was supported by the observation of the changes in the cross-peaks from the side chains of Pro9 (PGIS Pro215) and Arg13 (PGIS Arg219) of the peptide (Figure 6).

Finally, the details of the docking of U46619 with the helix F/G loop peptide were confirmed by the observation of the cross-peaks resulting from the interaction of U46619 with the particular individual residues of the peptide in the NOESY spectrum (Figure 7A). Comparing the NOESY spectra of the mixture of the F/G loop peptide and U46619 to that of only U46619 or the F/G loop peptide, two cross-peaks that only appeared in the spectrum of the mixture were identified as the intermolecular NOE between the peptide and U46619 (Figure 7). On the basis of their D1 and D2 chemical shifts, peak 1 arose from the short distance between H5 or H6 of U46619 (D1) and δ_1H_3 of Leu214 of the F/G loop peptide (D2); peak 2 arose from the short distance between CH_2 of U46619 (D1) and βH of Pro215 of the F/G loop peptide (D2). These results indicated that residues Leu214 and Pro215 within the F/G loop of PGIS interacted with U46619 (Figure 5). Thus, the residues in the PGIS F/G loop may be involved in forming the substrate access channel via the ER membrane and play an important role in the catalytic function of the membrane-bound PGIS.

Table 2: Comparison of the Activity of PGIS Mutants Expressed in COS-1 Cells Determined by TLC

Multiple mutation		Single mutation	
mutation site	PGIS activity relative to wild type (%)[a]	mutation site	PGIS activity relative to wild type (%)[a]
		L210M	120
LDR210−212MNK	30	D211N	50
		R212K	110
LP214−215QR	0	L214Q	20
		P215R	0
		K216A	110
KLA216−218ANP	0	L217N	60
		A218P	30
		R219D	40
RGS219−221DDP	20	G220D	100
		S221P	120
LSVG222−225AYDE	100		

[a] The activity of wild-type PGIS in the estimation of densities of 6-keto-PGF1α bands on TLC was set as 100%.

Localization of the Helix F/G Loop Residue(s) Important to Catalytic Function of the Membrane-Bound PGIS Using Site-Directed Mutagenesis. To test whether the 2-D NMR experimental approach used to identify the residues that interacted with U46619 is feasible, we have designed a set of recombinant mutant PGIS proteins to scan the F/G loop region for identification of the residues important for the enzyme activity.

The corresponding residues in the F/G loop of PGIS were changed to the residues of cytochrome P450BM3 based on the 3-D structural alignment (Figure 2B) using mutation approaches. To quickly scan the F/G loop region important to the enzyme activity, the first set of recombinant PGIS (Table 2) was created with multiple residue replacements using the PCR mutation approach described in the Materials and Methods. The recombinant PGIS proteins were expressed in COS-1 cells, and the molecular weight and similar expression levels were confirmed by Western blot (Figure 8) except for one recombinant PGIS with replaced residues of KLA216−218ANP that had a low expression level (Figure 8). The catalytic activities of the recombinant PGIS were evaluated by the enzyme assay starting with an addition of [^{14}C]-AA into the mixture of PGHS and cell homogenates containing recombinant PGIS. The product, [^{14}C]6-keto-$PGF_{1\alpha}$, was extracted and separated by TLC. The recombinant PGIS with the alteration of LP214−215QR corresponding to the residues on P450BM3 resulted in a significantly low level of production of 6-keto-$PGF_{1\alpha}$ that hydrolyzed from PGI_2, reflecting the amount of PGI_2 converted from PGH_2 (Figure 9). The catalytic activities of the LDR210−212MNK

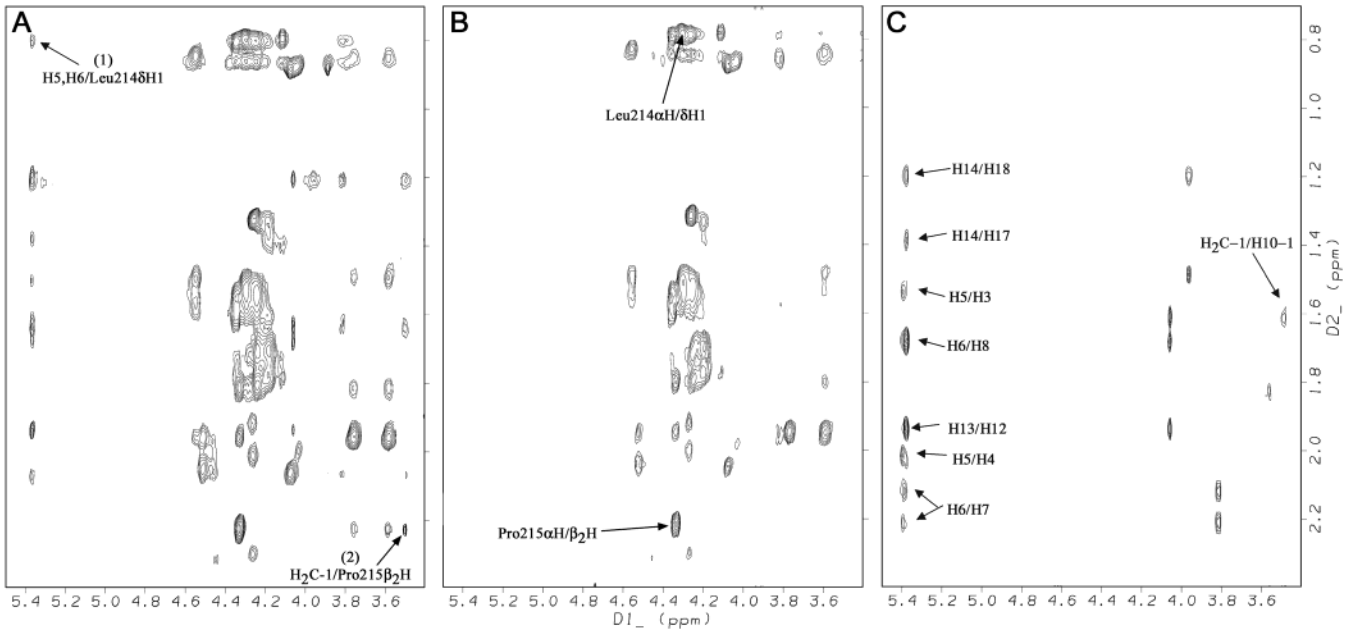

FIGURE 7: Expanded region of the NOESY spectra of the F/G loop with U46619 (A), without U46619 (B), and U46619 only (C). The extra cross-peaks were identified as the interaction of the F/G loop peptide with U46619: (1) H5 or H6 of U46619 and δ_1H_3 of Leu214 of the F/G loop and (2) CH_2 of U46619 and βH of Pro215 of the F/G loop.

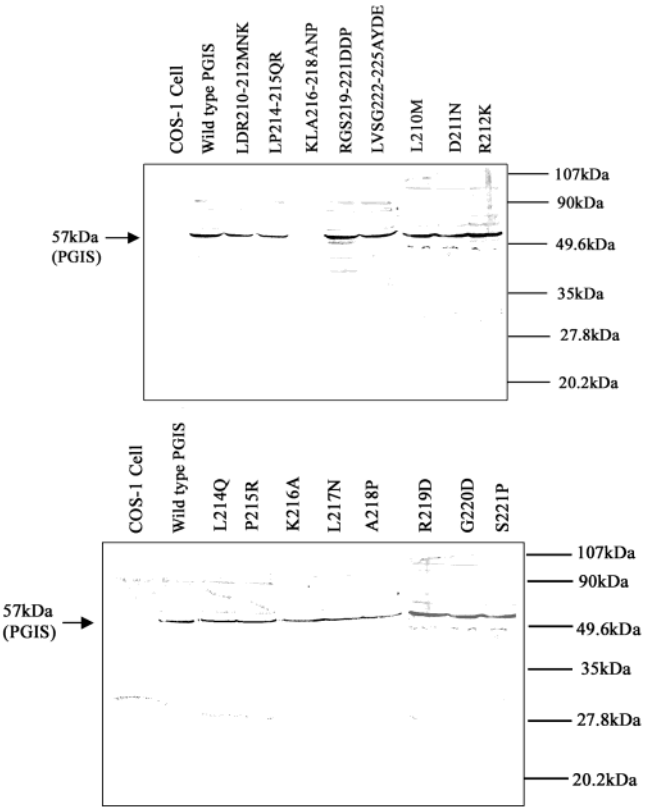

FIGURE 8: Western blotting analysis of expression of PGIS wild-type and mutants in COS-1 cells. A 60 μg sample of transfected or nontransfected COS-1 cell protein, separated by SDS 10%-(w/v)-PAGE, was transferred on to a nitrocellulose membrane. The membrane was probed with rabbit polyclonal anti PGIS peptide (residues 472−482) antibody (*1*). The positions of molecular-mass standard were shown on the right side. The arrow on the left side shows the position of PGIS protein.

and RGS219−221DDP mutations were diminished ambiguously. In contrast, the LSVG222−225AYDE mutants retained a significant fraction of the wild-type enzymatic activity (Figure 9). Furthermore, the residues in the PGIS F/G loop, which showed that activity changes significantly or ambiguously by the multiple residues replacement mutation, were selected for point mutation to further localize the individual residue important to the enzyme activity. The recombinant PGIS proteins with point mutations at residues L210M, D221N, R212K, L214Q, P215R, K216A, L217N, A218P, R219D, G220D, and S221P were constructed, expressed, and assayed as described above (Table 2, Figure 9). The catalytic activity of the recombinant PGIS was significantly diminished by the point mutation at L214Q and P215R when compared to the wild type PGIS (Figure 9). The conclusion of the localization of the key residues important to the membrane-bound PGIS activity in the F/G loop region are the same as the observations from the 2-D NMR experiment using the synthetic peptide to interact with U46619. This result indicated that the 2-D NMR experiment could be used as a guide for point mutagenesis to quickly localize the residues important to the biological function of the enzyme. This 2-D NMR experiment-guided mutagenesis approach will be useful for structural and functional studies for other proteins.

DISCUSSION

Our studies of the topology of the NH_2-terminal solution structure and the overall structure of PGIS using site-specific peptide antibodies, CD, 2-D NMR experiments, and molecular modeling (*1*, 7, *8*, *21*) have allowed us to hypothesize a membrane-bound topological arrangement for PGIS. In this arrangement, the large cytoplasmic domains are anchored to the ER membrane by the NH_2-terminal membrane anchor domain and a putative membrane contact region located in the helix F/G loop (Figure 1). This model is consistent with fluorescence energy transfer studies, which indicate the distance between the heme of P450 and the membrane surface is about 50 Å (*22*). Our hypothesis for the involvement of the PGIS helix F/G loop in membrane contact has been indirectly supported by recent protein engineering and crystallographic studies for a recombinant mutant microsomal

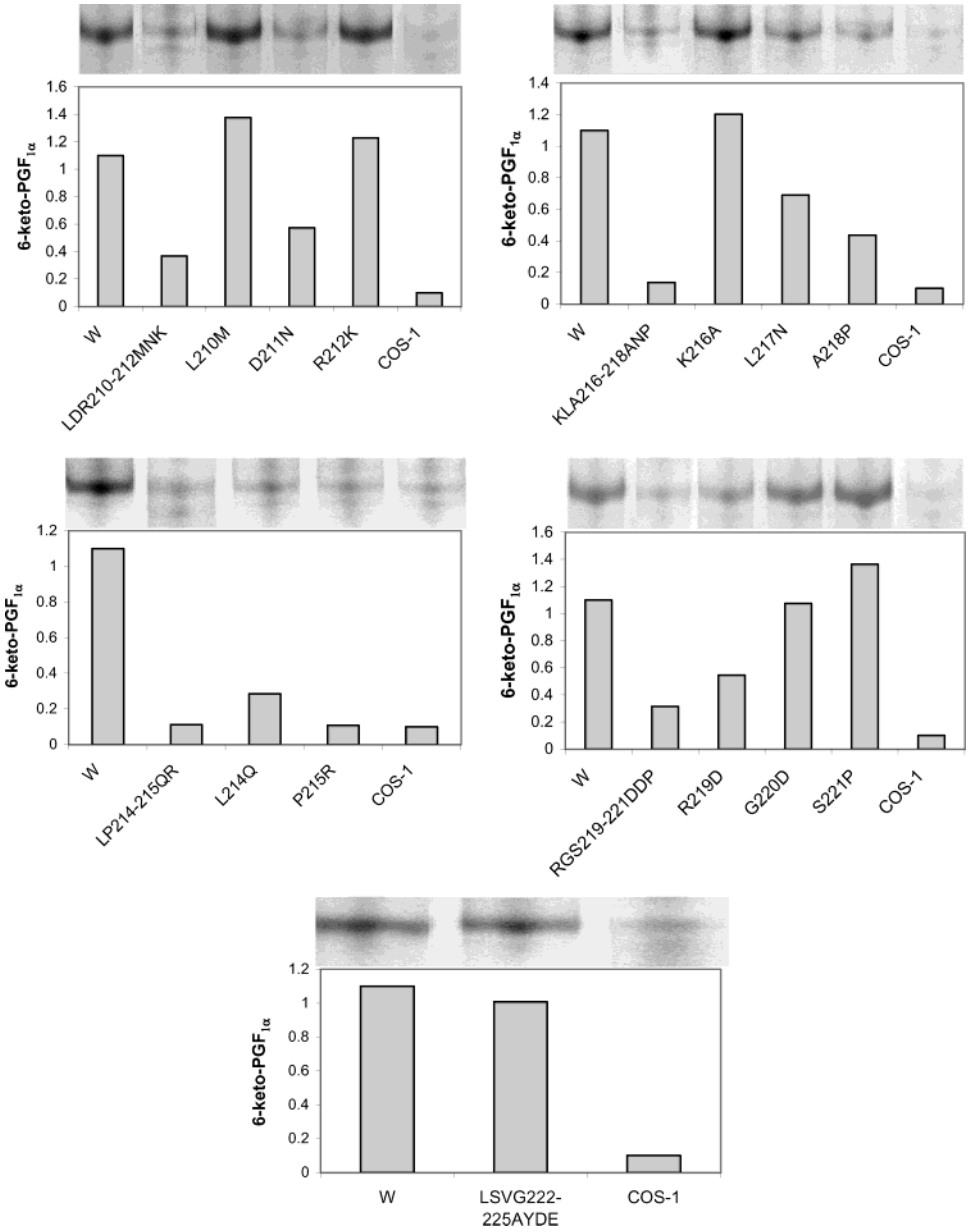

FIGURE 9: Autoradiogram of PGIS activity assay using the TLC method. The enzyme activity assay and the TLC procedure were described in the Materials and Methods. The bands of [^{14}C] labeled 6-keto-PGF$_{1\alpha}$ produced from [^{14}C]-AA by PGIS or PGIS mutants were shown under the autoradiograph (top) and plotted (bottom) depending on the density of each band.

P450 2C5, in which the membrane-bound P450 became soluble after deletion of the NH_2-terminal membrane anchor domain and modification of the F/G loop residues (*23*, *24*). Crystallographic studies of detergent-solubilized PGHS-1 and -2 suggest that the catalytic domains of the proteins lie on the luminal side of the ER, anchored to the ER membrane by hydrophobic side chains of amphipathic helices A−D. These hydrophobic side chains of the putative membrane anchor domains also form an entrance to the substrate-binding channel and potentially form an initial docking site for the lipid substrate, AA (*25*, *26*). The topology models developed for PGIS described above have their catalytic domains on the cytoplasmic site of the ER, opposite to the orientation for PGHS. The substrate channels of the two enzymes open at or near the ER membrane surface. This suggests that the coordination between PGHS and PGIS in the biosynthesis of PGI_2 is facilitated by the enzyme's anchoring to the lipid membrane. The coordination model raises an important question of whether the presentation of PGH_2 to the active sites of PGIS is affected by the PGIS helix F/G loop residues that surround the substrate access channel in the membrane-bound enzyme. Thus, identification of PGIS F/G loop residues important to the interaction with PGIS substrate is critical to the understanding of the structural and functional relationships in the coordination between PGHS and PGIS in the native membrane environment.

Synthetic peptides have emerged as important tools in characterizing the functional domains of proteins including PGIS (*27*−*31*). Synthetic peptides mimicking the portion of the native proteins determined by NMR spectroscopy technique have become a useful approach to understanding the protein function at the 3-D structural level (*32*−*36*). A loop peptide approach whose peptide termini are constrained to a limited separation distance is presumably more likely to mimic the native loop structure than the corresponding peptide with unrestricted ends. This approach has been

successfully tested with a cyclic peptide corresponding to the second extracellular loop (residues 173−193) of the thromboxane A_2 receptor (TP) in which the N- and C-termini are connected by a homocysteine disulfide bond (*19*). The constrained TP peptide showed biological activity binding to the receptor ligand and displayed a defined 3-D structure by 2-D NMR experiments (*19*). The distance between the N- and C-termini of the receptor peptide shown in NMR structure is 14.23 Å, which matched the distance (14.51 Å) between the two transmembrane helices that connected the second extracellular loop in the TP receptor model. This suggests that the approach using cyclic peptides greatly increases the ability to mimic the functional domain of proteins and the likelihood of solving the 3-D structure of the functional domain of protein. This approach was used to design and synthesize the PGIS F/G loop peptide (Figure 2A). The binding of the peptide to the PGIS substrate analogue, U46619, has been observed by 2-D NMR experiments (Figure 7), which further supports the use of the constrained peptide approach to mimic a protein segment for functional and structural studies.

The described ^{1}H 2-D NMR experiments for the interaction of the constrained F/G loop peptide in the presence of U46619 provided detailed information about the analogue contacted with the residues in the peptide. Whether the residues contacted with U46619 identified by the NMR experiment can apply to the native PGIS protein, point mutation for the residues in the native PGIS shall give an answer. The recombinant PGIS proteins with point or multiple mutation approach within the F/G loop region were used to confirm the observation from the 2-D NMR experiments using the constrained F/G loop peptide. Localization of the residues in the F/G loop important to PGIS catalytic function using the 2-D NMR experiments and the mutation scanning method showed identical results. This finding supported the observation of the interaction between the F/G loop peptide and U46619 using 2-D NMR experiments. Thus, the information obtained from the NMR studies using the constrained peptide could be used to guide mutagenesis studies for the protein. In this case, the time-consuming scanning mutation can be avoided. We call this combined 2-D NMR experiment and mutagenesis approach as a 2-D NMR experiment-guided mutagenesis method. This method can be applied to the identification of functional residues for other P450s and proteins.

Identification of the residues in the F/G loop important to the catalytic function of the membrane-bound PGIS by combination of 2-D NMR experiments and recombinant proteins was first reported here, which allowed us to refine the topological model of the native PGIS in respect to the ER membrane and the substrate access channel (Figure 10). It clearly showed that the two identified residues are on the way of the substrate while accessing to its heme binding pocket (Figure 10). This finding provided direct evidence to support our previous conclusion using site-specific antibodies (*1*), in which the PGIS substrate access channel opening, formed by part of the F/G loop residues, is found to be up against the ER membrane (ref *1*, Figure 10), and the F/G loop is involved in influencing the substrate access channel formation of the membrane-bound PGIS. In this case, once the hydrophobic PGH_2 produced by PGHS is dissolved

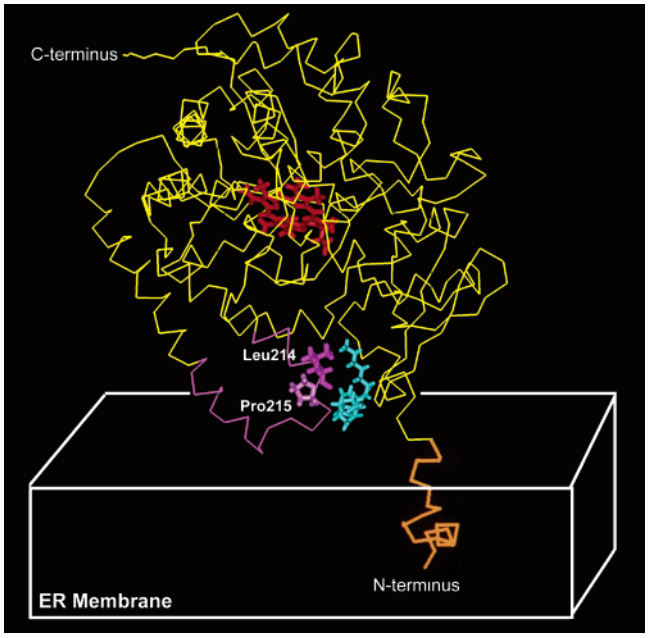

FIGURE 10: Refined topological model of the native PGIS (yellow) in respect to the ER membrane with the NMR structures of the bound form of F/G loop (magenta) and the NH_2-terminal segment (orange) connected. The identified residues (Leu214 and Pro215) that contacted with U46619 as described in Figure 5 were displayed. U46619 (blue) was placed in the position of the substrate access channel based on the orientation shown in Figure 5. Red denotes heme.

in ER membrane, it can enter the active site of the membrane-bound PGIS efficiently without having to contact the solvent. This predicts that the efficiency of eicosanoid biosynthesis will be different in the soluble and the membrane-bound enzymes. One indication of such a difference was reported from Eling et al. (*37*), who found channeling of AA through PGG_2 to PGH_2 in microsomal PGHS but not in detergent-solubilized PGHS. Other observations, which support the hypothesis, are that PGH_2 has a longer half-life in lipid than in a solvent environment and that cyclooxygenase side products are much less plentiful in biosynthesis of PGI_2 with intact membrane-bound systems than solubilized enzymes. This suggests that the lipid substrate, PGH_2, has higher-efficiency access to the active sites and is less likely to degrade in the membrane-bound systems.

Overall, the findings from these studies are important for understanding the structure/function relationship of PGIS in the biosynthesis of PGI_2 and its coordination with PGHS during prostanoid biosynthesis in the native ER membrane environment. The information described 2-D NMR-experiment-guided mutagenesis method is also useful for structure/function relationship studies of other proteins.

ACKNOWLEDGMENT

We thank Dr. Xialian Gao from the Chemistry Department of the University of Houston for providing the NMR instrument and help on taking the 2-D NMR spectra. An acknowledgment is also made to the Robert A. Wetch Foundation (E-1270) and the W. M. Keck Center for Computational Biology for computer resource support. We also thank Ms. Lori Jenkins for the manuscript editing assistance.

REFERENCES

1. Deng, H., Huang, A., So, S. P., Lin, Y. Z., and Ruan, K. H. (2002) *Biochem. J. 362*, 545−551.
2. Moncada, S., and Vane, J. R. (1978) *Pharmacol. Rev. 30*, 293−331.
3. Wu, K. K., and Thiagarajan, P. (1996) *Rev. Med. 47*, 315−331.
4. Pico, D., Loll, P. J., and Garavito, R. (1994) *Nature 367*, 243−249.
5. Ren, Y., Walker, C., Loose-Mitchell, D. S., Deng, J., Ruan, K. H., and Kulmacz, R. J. (1995) *Arch. Biochem. Biophys. 323*, 205−214.
6. Otto, J. C., and Smith, W. L. (1994) *J. Biol. Chem. 269*, 19868−19875.
7. Lin, Y. Z., Wu, K. K., and Ruan, K. H. (1998) *Arch. Biochem. Biophys. 352*, 78−84.
8. Lin, Y. Z., Deng, H., and Ruan, K. H. (2000) *Arch. Biochem. Biophys. 379*, 188−197.
9. Wüthrich, K. (1986) *NMR of Proteins and Nucleic Acids*, pp 44−92, John Wiley & Sons, Inc., New York.
10. Englander, S. W., and Wand, A. J. (1987) *Biochemistry 26*, 5953−5958.
11. Chazin, W. J., Rance, M., and Wright, P. E. (1988) *J. Mol. Biol. 202*, 603−622.
12. Basus, V. J. (1989) *Methods Enzymol. 177*, 132−149.
13. So, S. P., Li, D., and Ruan, K. H. (2000) *J. Biol. Chem. 275*, 40679−40685.
14. Braunschweiler, L., and Ernst, R. R. (1983) *J. Magn. Reson. 53*, 521−528.
15. Bax, A., and Davis, D. G. (1985) *J. Magn. Reson. 61*, 306−320.
16. Jeener, J., Meier, B. H., Bachmann, P., and Ernst, R. R. (1979) *J. Chem. Phys. 71*, 4546−4553.
17. Wu, J., So, S. P., and Ruan, K.-H. (2003) *Arch. Biochem. Biophys. 411*, 27−35.
18. Ruan, K. H., Li, D. W., Ji, J., Lin, Y. Z., and Gao, X. L. (1998) *Biochemistry 37*, 822−830.
19. Ruan, K. H., So, S. P., Wu, J., Li, D., Huang, A., and Kung, J. (2001) *Biochemistry 40*, 275−280.
20. Ruan, K. H., So, S. P., Zheng, W., Wu, J., Li, D., and Kung, J. (2002) *Biochem. J. 368*, 1−7.
21. Shyue, S. K., Ruan, K. H., Wang, L. H., and Wu, K. K. (1997) *J. Biol. Chem. 272*, 3657−3662.
22. Centeno, F., and Gutierrez-Merino, C. (1992) *Biochemistry 31*, 8473−8481.
23. Williams, P., Sridhar, V., and McRee, D. E. (1999) 11th International Conference on Cytochrome P450, Sendai, Japan, pp 19, L3.
24. Johnson, E. F., Cosme, J., Williams, P., and McRee, D. E. (1999) 11th International Conference on Cytochrome P450, Sendai, Japan, pp 18, L2.
25. Pico, D., Loll, P. J., and Garavito, R. M. (1994) *Nature 367*, 243−249.
26. Kurumbail, R. G., Stevens, A. M., Gierse, J. K., McDonald, J. J., Stegeman, R. A., Pak, J. Y., Gildehaus, D., Miyashiro, J. M., Penning, T. D., Seibert, K., Isakson, P. C., and Stallings, W. C. (1996) *Nature 384*, 644.
27. Franzoni, L., Nicastro, G., Pertinhez, T. A., Tato, M., Nakaie, C. R., Paiva, A. C. M., Schreiner, S., and Spisni, A. (1997) *J. Biol. Chem. 272*, 9734−9741.
28. Anand-Srivastava, M. B., Sehl, P. D., and Lowe, D. G. (1996) *J. Biol. Chem. 271*, 19324−19329.
29. Grasso, P., Leng, N., and Reichert, L. E., Jr. (1995) *Mol. Cell. Endocrinol. 108*, 43−50.
30. Dias, J. A. (1996) *Mol. Cell. Endocrinol. 125*, 45−54.
31. Koke, H. K., Liotta, A. S., Kole, S., Roth, J., Montrose-Rafizadeh, C., and Bernier, M. (1996) *J. Biol. Chem. 271*, 31619−31626.
32. Yeagle, P. L., Alderfer, J. L., and Albert, A. D. (1995) *Nat. Struct. Biol. 2*, 832−834.
33. Yeagle, P. L., Alderfer, J. L., and Albert, A. D. (1995) *Biochemistry 34*, 14621−14625.
34. Yeagle, P. L., Alderfer, J. L., and Albert, A. D. (1996) *Mol. Vis. 2*, 12.
35. Yeagle, P. L., Alderfer, J. L., Salloum, A. C., Ali, L., and Albert, A. D. (1997) *Biochemistry 36*, 3864−3869.
36. Yeagle, P. L., Alderfer, J. L., and Albert, A. D. (1997) *Biochemistry 36*, 9649−9654.
37. Eling, T. E., Glasgow, W. C., Curtis, J. F., Hubbard, W. C., and Handler, J. A. (1991) *J. Biol. Chem. 266*, 12348−12355.

BI026749Z